Jointly published by
Akadémiai Kiadó, Budapest
and Kluwer Academic Publishers, Dordrecht

React.Kinet.Catal.Lett.
Vol. 76, No. 1, 83-92
(2002)

RKCL4070

CATION/ANION MODIFIED CERIA-ZIRCONIA SOLID SOLUTIONS PROMOTED BY Pt AS CATALYST OF METHANE OXIDATION INTO SYNGAS BY WATER IN REVERSIBLE REDOX CYCLES

V.A. Sadykov[a,b], T.G. Kuznetsova[a], S.A. Veniaminov[a], D.I. Kochubey[a], B.N. Novgorodov[a], E.B. Burgina[a], E.M. Moroz[a], E.A. Paukshtis[a,b], V.P. Ivanov[a], S.N. Trukhan[a], S.A. Beloshapkin[a], Yu.V. Potapova[a], V.V. Lunin[c], E. Kemnitz[d] and A. Aboukais[e]

[a]Boreskov Institute of Catalysis, Novosibirsk 630090, Russia;
[b]Novosibirsk State University, Novosibirsk 630090, Russia,
[c] Lomonosov Moscow State University, Chemical Department, Moscow 119899, Russia;
[d]Institute for Chemistry, Humboldt-University, Berlin, Germany;
[e]Laboratoire de Catalyse et Environement MREID, Université du Littoral-Cote d'Opale, Dunkerque, France

Received February 7, 2002
Accepted February 20, 2002

Abstract

Ca and/or F-modified fluorite-like Ce-Zr-mixed oxides have been prepared by Pechini's method. The bulk structure of samples was characterized by XRD, EXAFS and FTIRS of the lattice modes. The surface properties were studied by SIMS and FTIRS of adsorbed CO and surface hydroxyls. The specific reactivity of the surface oxygen, its amount, coefficients of bulk and near-surface diffusion, as dependent upon the sample composition and temperature, were estimated using sample reduction by CO in the pulse/flow mode. Insertion of fluorine into the lattice results in decreasing the degree of oxygen polyhedra distortion, thus decreasing the amount of reactive oxygen and diffusion coefficients. Calcium and Pt addition counteracts this effect. At 500^{o}C for Pt-supported Ce-Zr-O samples including those modified by Ca and F, the lattice oxygen is easily removed by methane generating CO and hydrogen with high selectivity. Reoxidation of reduced samples by water or carbon dioxide at the same temperature restores the oxygen capacity producing more hydrogen or carbon monoxide.

Keywords: Ceria-zirconia solid solution, methane oxidation into syngas, reactivity of lattice oxygen, surface and bulk diffusion, effect of bulk and surface promoters

0133-1736/2002/US$ 12.00.

INTRODUCTION

Selective partial oxidation of methane into syngas (CO and H_2) is now considered as one of the promising ways of methane utilization. However, the air separation equipment required to produce pure oxygen is rather expensive, thus decreasing the efficiency of technology. To overcome this problem, the selective methane oxidation by lattice oxygen of the oxide catalyst (CeO_2 with admixed Pt) was suggested [1,2]. However, design of those oxide systems with a high oxygen capacity and mobility combined with the lattice stability in reversible redox cycles remains a problem. Ceria-zirconia solid solutions possessing a high lattice oxygen mobility and storage capacity successively applied in automotive catalysis [3] appear to be a promising option, though they have not yet been tested for the unsteady-state processes of methane conversion into syngas.

This work aims at the synthesis of ceria-zirconia based solid solutions and checking the ability of their lattice oxygen to efficiently transform methane into syngas in reversible redox cycles. To ensure the high dispersion of complex oxides along with their phase purity and homogeneous distribution of components in the lattice, samples were synthesized by the Pechini method [4] not applied earlier for those systems. To control the surface/lattice oxygen mobility and reactivity, samples were modified by incorporation of Ca cations and F anions into the lattice, while Pt was supported on their surface to enhance the rate of methane transformation. To elucidate factors determining the amount, mobility and reactivity of the surface/lattice oxygen estimated using sample reduction by CO and methane, some basic structural features and surface composition were estimated using X-ray powder diffraction, EXAFS, FTIRS of lattice modes and SIMS.

EXPERIMENTAL

For the sample synthesis *via* the Pechini route, corresponding salts (cerium nitrate zirconyl chloride, calcium fluoride) in the required ratios were added at 60^{o}C to a solution of citric acid in ethylene glycol (1:4 mole ratio) while the Me : citric acid ratio was equal to 1:2. The solution heating was accompanied by the increase in its viscosity followed by solidification and self-ignition. Calcination of a residue at 800^{o}C allows obtaining the mixed oxide samples with a reasonably high specific surface area. Fluorinated samples were obtained either by adding CaF_2 to the salts solution, or by heating mixed oxide samples with solid ammonium fluoride [5] at 220^{o}C for 6 hours followed by annealing at 500^{o}C for 1 h. The samples loaded with Pt (1.4 wt.%) were prepared by incipient wetness impregnation with a H_2PtCl_6 solution followed by calcination

at 700°C for 2 hours.

Infrared spectra of the samples in the 220-4000 cm^{-1} were registered using a BOMEM M 102 spectrometer.

X-ray powder diffraction patterns were recorded using monochromatized CuKα radiation and a URD-63 diffractometer.

EXAFS spectra of Zr K-edge were obtained at the EXAFS station of the Siberian Center of Synchrotron Radiation, Novosibirsk, in a standard transmission mode. The data were analyzed as $k^3c(k)$ in the range of wave numbers k = 3-13 $Å^{-1}$. The interatomic distances, coordination numbers and the Debye-Waller factors were obtained by spectra modeling with the EXCURV92 program.

The surface chemical composition was analyzed with the SIMS method using an MS-7201 mass-spectrometer. The energy of the incident Ar^+ ion beam was equal to 4 keV, with the current density 10-20 $\mu A/cm^2$. To prevent sample charging during the ion bombardment, the samples were supported onto a high purity indium foil.

Sample reduction by CO (1% CO in a He mixture) in the pulse and flow modes was carried out using a microcatalytic installation and a reactor with the vibrofluidized bed of the catalyst (catalyst weight 10-100 mg). Before the reduction, the samples were pretreated in the oxygen flow at 500°C for 1 h. All gases were purified by passing through traps which are cooled by liquid nitrogen. The reaction mixtures were analyzed by GC with a thermal conductivity detector. The reduction rates were calculated using an equation for the ideal mixing reactor [6]. In each experiment, the sample was first reduced by pulses of CO in He (pulse volume 9.8 cm^3) and then in the flow of the reducing mixture. The sample reduction degree was expressed in monolayers (1 monolayer = 10^{19} atoms/m^2).

Methane selective oxidation into syngas by the lattice oxygen of the Pt-promoted catalysts was carried out in a flow regime using a diluted mixture of 0.1 % CH_4 in He. Before the experiments, the samples were pretreated in the O_2 flow at 500°C for 2 h. In some experiments, after the reduction, the samples were reoxidized in the flow of either 0.6 % of H_2O or 0.5 % CO_2 in He followed by repeated reduction by methane. GC was used to analyze the reagent and product concentrations.

RESULTS AND DISCUSSION

Bulk and surface properties of the samples

According to the XPD data, for the Ce-Zr-O samples synthesized by the

Pechini method (Table 1), the diffraction peaks typical for ceria with a fluorite-

Table 1

Some structural data for ceria-zirconia based solid solutions

Sample	Specific surface (m^2/g)	Phase composition*	EXAFS parameters[a]			
			Scattering element	R	N	σ^2, Å^2
$Ce_{0.5}Zr_{0.5}O_2$	16	CeO_2 (ZrO_2)	Zr-O	2.13	5.1	0.017
		a = 5.39 Å	Zr-Zr(Ce)	3.67	2.2	0.007
$Ce_{0.8}Zr_{0.2}O_{1.8}F_x$	20	CeO_2 (CeF_3)	Zr-O	2.18	4.7	0.009
		a = 5.38 Å	Zr-F	2.03	2.1	0.005
			Zr-Ce	3.55	0.7	0.005
$Ce_{0.6}Zr_{0.2}Ca_{0.2}O_{1.8}F_x$	15	CeO_2,	Zr-O	2.27	2.6	0.010
		(ZrO_2, CaF_2)	Zr-F	2.10	2.2	0.004
		a = 5.38 Å	Zr-Ce	3.53	1.7	0.011

* Admixed phases indicated in parenthesis

[a] R is the distance; N is the coordination number; σ^2 is the Debye-Waller factor

type structure (JCPDS 43-1002) were registered. As judged by the diffraction peak broadening, a mean particle size is in the range of 100-130 Å. As compared with a pure ceria phase (a = 5.412 Å), the lattice parameter for the Ce-Zr-O samples including those modified by Ca and/or F was decreased (Table 1), thus evidencing Zr incorporation into the lattice [7]. For the $Ce_{0.5}Zr_{0.5}O_2$ sample, the low intensity diffraction peaks were registered as well, which can be assigned either to ZrO_2 (JCPDS 42-1164) or to the $Ce_{0.15}Zr_{0.85}O_{1.85}$ solid solution (JCPDS 17-923). For the $Ce_{0.8}Zr_{0.2}O_{1.8}F_x$ sample obtained via the gas-phase fluorination, an admixture of the CeF_3 phase (JCPDS 08-0045) was detected, thus evidencing an excess fluorination. For the $Ce_{0.6}Zr_{0.2}Ca_{0.2}O_{1.8}F_x$ sample, along with the CeO_2-like cubic phase, a weak diffraction maximum corresponding to CaF_2 (JCPDS 35-816) was observed. After Pt supporting on $Ce_{0.5}Zr_{0.5}O_2$ and $Ce_{0.6}Zr_{0.2}Ca_{0.2}O_{1.8}F_x$, the additional diffraction peaks corresponding to metallic Pt with the mean particle size *ca.* 400 Å appear.

Hence, the Pechini method allows to synthesize the dispersed rather homogeneous mixed Ce-Zr oxides including those promoted by Ca and F.

The EXAFS data (Table 1) allow tracing the sample structure variation due to incorporation of guest cations (Ca) and fluorine into the lattice. The fluorine addition is accompanied by an increase in the integral Zr-anion coordination

number and a decrease in the corresponding Debye-Waller factor. It suggests that fluorine addition leads to a decrease in the local disordering of the oxygen coordination polyhedra. The addition of Ca decreases the integral Zr-anion coordination number and increases the disordering, which is explained by an effect of anion vacancies generated by addition of that cation. The Zr-O distances are increased as well, which evidences weakening of the corresponding bonds due to the disordering.

The FTIRS data on the lattice modes (not shown here for brevity) agree with the EXAFS data. For pure ceria, in the range of the lattice modes, a broad band with a maximum at ~390 cm^{-1} dominates. A weak shoulder at ~500 cm^{-1} indicative of the oxygen polyhedra distortion in the hydroxyls-containing sample is observed as well. Incorporation of Zr into the lattice makes a shoulder at ~500 cm^{-1} more developed due to a stronger distortion of the oxygen polyhedra around zirconia cations [8].

Fluorination of the solid solution (the $Ce_{0.8}Zr_{0.2}O_{1.8}F_x$ sample) decreases the intensity of a shoulder at ~550 cm^{-1}, while the main band is slightly shifted to higher frequencies. These changes suggest a decrease in the oxygen environment distortion due to the fluorine incorporation.

The calcium incorporation into the lattice is reflected by a broadening of the main absorption band and enhancing the shoulder intensity due to the generation of anion vacancies.

Pt supporting increases further the intensity of the shoulder at ~500 cm^{-1} which can be explained by the incorporation of the Pt cations. Indeed, appearance of oxidized Pt species (the Pt cations and/or platinum oxide patches) was directly proved for Pt supported onto ceria-alumina by using such methods as Laser Raman Spectroscopy [9] and FTIRS of the adsorbed CO test molecules [10].

Table 2

Ratios of the SIMS ion currents for the main components of ceria-zirconia based solid solutions

Sample	Surface			Bulk		
	$Zr^+/{}^+Ce$	Ca^+/Ce^+	$(CeOH_3^+ + CeF^+)/Ce^+$	Zr^+/Ce^+	Ca^+/Ce^+	$(CeOH_3^+ + CeF^+)/Ce^+$
$Ce_{0.5}Zr_{0.5}O_2$	0.05	-	-	0.16	-	-
$Ce_{0.8}Zr_{0.2}O_{1.8}F_x$	0.11	-	0.8	0.17	-	1.5
$Ce_{0.6}Zr_{0.2}Ca_{0.2}O_{1.8}F_x$	0.13	15	0.2	0.1	3	0.2
$Pt/Ce_{0.5}Zr_{0.5}O_2$	0.06	-	-	0.08	-	-
$Pt/Ce_{0.6}Zr_{0.2}Ca_{0.2}O_{1.8}F_x$	0.08	3.0	0.02	0.09	1.0	0.03

Some data on the surface composition of the samples estimated by SIMS are presented in Table 2. The most important feature is that the surface appears to be depleted of Zr and fluorine and enriched with Ca, as follows from comparison of the ratio of ion currents corresponding to the surface layer and the bulk of the samples. Note that the ratio of Zr^+/Ce^+ ion currents in the bulk depends not only on the content of those elements, but also on that of fluorine. It is explained by the effect of fluorine on the relative ease of cation sputtering due to a variation of the cation-anion coordination numbers as well as of the strength of corresponding bonds. Though these data will be discussed in detail elsewhere, this conclusion agrees well with the results obtained by the other methods (see above). In the fluorinated samples, the cerium cations seem to have a more dense coordination sphere with the stronger bonds as compared with the Zr cations. Pt supporting certainly affects the spatial distribution of the other components making it more uniform.

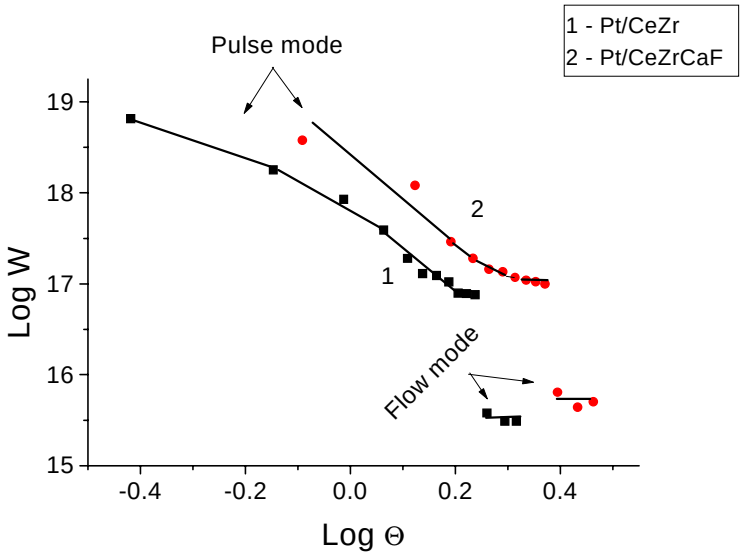

Fig. 1. Log-log dependence of the reduction rate W (molecules CO/m^2 s) *vs.* degree of the surface reduction Θ (monolayers) in the pulse and flow modes for Pt-supported ceria-zirconia based solid solutions $Ce_{0.5}Zr_{0.5}O_2$ (curve 1) and $Ce_{0.6}Zr_{0.2}Ca_{0.2}F_xO_y$ (curve 2). 1% CO in He, 500°C

Oxygen mobility

Typical reduction curves are presented in Fig. 1. According to [11], the decrease in the reduction rate is explained by a consumption of the reactive surface oxygen. In the pulse regime, after a certain amount of oxygen is removed from the surface, the reduction rate is constant. It means that the surface coverage by reactive oxygen (or surface reduction degree θ_{st}) becomes independent of the pulse number due to replenishing of oxygen removed from the surface by each pulse of CO ($\Delta\theta$). This replenishing goes through an oxygen «leakage» from the subsurface layer during the period of relaxation between the pulses ($\tau \sim 420$ s) when a sample is kept in the stream of He. This process is characterized by the diffusion exchange constant V_D [11]. This value can be estimated assuming the first order law of oxygen diffusion from the subsurface layer, which yields the integral relation $V_D = -\{\ln [\theta_{st}/(\theta_{st} + \Delta\theta)]\}/\tau$.

When the oxide is reduced in the flow regime, another region with an approximately constant reduction rate for 30-60 min appears. In this case, oxygen removal from the surface by CO is compensated by the oxygen diffusion from the bulk characterized by the coefficient of the bulk oxygen diffusion D. The latter quantity is estimated from Fick's first law using the measured values of the sample reduction rate, the maximum surface reduction degree corresponding to transformation of all cerium cations into the 3+ state and known values of the oxygen bulk concentration.

Table 3

Some characteristics of the oxygen mobility and reactivity of ceria-based systems at 500°C

Sample	W_{sp} [a] (s^{-1})	N_o [b] (% monol)	V_D [c] (s^{-1})	D [c] ($10^{-21} m^2 s^{-1}$)	E_a [e] (kJ/mol)	
					near-surface	bulk
$Ce_{0.5}Zr_{0.5}O_2$	0.07	64.5	2.3	11.4	16	6
$Pt/Ce_{0.5}Zr_{0.5}O_2$	0.70	129	1.3	3.4	9	6
$Ce_{0.8}Zr_{0.2}O_{1.8}F_x$	0.04	2.4	3.7	0.1	2	-
$Pt/Ce_{0.6}Zr_{0.2}Ca_{0.2}O_{1.8}F_x$	0.2	225	1.1	5.5	0	0

[a] specific surface reduction rate according to [11];
[b] amount of surface reactive oxygen easily removed by CO pulses at 500°C;
[c] effective rate constant of oxygen diffusion exchange between the surface and the first subsurface layer [11];
[d] coefficient of bulk oxygen diffusion

The values of those parameters along with the corresponding activation energies estimated in the range of 300-500°C are presented in Table 3. The magnitudes of V_D and D agree reasonably with those earlier obtained for oxide systems with a substantial near-surface (CuO [11]) and bulk (CeO_2 [12]) diffusion. The low activation energies of the oxygen bulk and near-surface diffusion agree with the earlier published data as well [13]. Though a more detailed analysis of these results will be presented elsewhere, some comments on the effects of the cation and anion modification of the ceria-based solid solutions can be made. Fluorine certainly decreases the surface oxygen reactivity $W_{sp.}$, its coverage N_o and lattice oxygen mobility D, which can be explained by the decrease in the coordination polyhedra disordering (see above). However, the rate constant V_D for the near-surface oxygen exchange is somewhat increased, thus indicating a complex rearrangement of the surface layer to be studied further. The Pt supporting increases the amount of reactive oxygen easily removed from the surface before reaching the first diffusion plateau, and only a part of this oxygen is bound to Pt. Hence, Pt activates the surface. However, it decreases the diffusion coefficients, probably, due to Pt cation incorporation into the surface layer (see above). Simultaneous incorporation of fluorine and calcium into the lattice and supporting Pt increases further the amount of reactive oxygen and bulk diffusion coefficients.

Oxidative transformation of methane

In the temperature range studied (up to 500°C), the samples without supported Pt were shown to be only weakly active in the deep oxidation of methane. The Pt supporting sharply enhances the catalyst performances and makes the samples selective in the syngas generation, which can be explained by an efficient C-H bonds activation on Pt. Some typical data for the $Pt/Ce_{0.6}Zr_{0.2}Ca_{0.2}O_{1.8}F_x$ sample are shown in Fig. 2. Similar results were obtained for the $Pt/Ce_{0.5}Zr_{0.5}O_2$ sample. As the reduction proceeds, methane conversion declines slowly, while the product selectivities vary faster: Selectivity toward CO_2 falls rapidly, while that of CO increases. Hydrogen selectivity not shown here for brevity, usually follows that of CO ($H_2/CO = 2$). These trends imply that weakly bound surface oxygen is responsible for the methane deep oxidation, while the lattice oxygen is involved in the syngas generation. Indeed, for two Pt-containing samples considered here, the amount of weakly bound oxygen determined by the CO pulse titration (*ca.* 1.3 and 2.3 monolayers for $Pt/Ce_{0.5}Zr_{0.5}O_2$ and $Pt/Ce_{0.6}Zr_{0.2}Ca_{0.2}O_{1.8}F_x$, respectively) correlates well with the amount of oxygen consumed for methane deep oxidation (*ca.* 1.2 and 1.9 monolayers, respectively). The amount of lattice

oxygen easily converted into syngas at 500°C corresponds to the range of methane conversion from 100% to *ca.* 10% and is equal for $Pt/Ce_{0.6}Zr_{0.2}Ca_{0.2}O_{1.8}F_x$ and $Pt/Ce_{0.5}Zr_{0.5}O_2$ samples to ca. 4.0 and *ca.* 2.2 monolayers, respectively. This correlates with the oxygen bulk diffusion coefficients (Table 3).

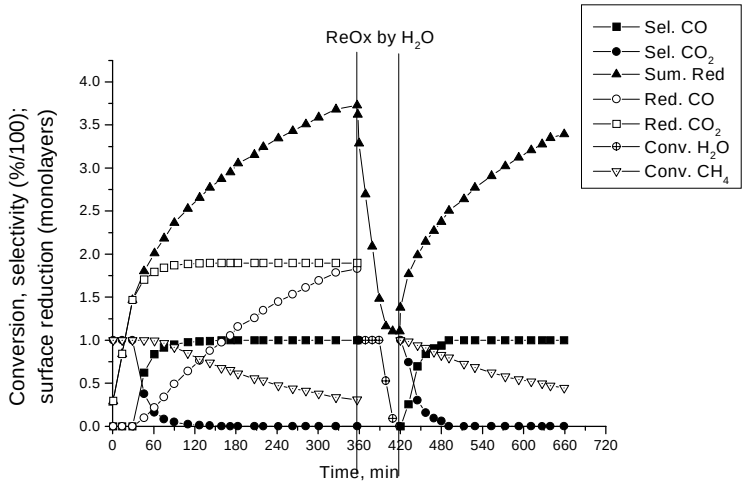

Fig. 2. Redox cycles: methane (0.1 %) – H_2O (0.6 %) – methane (0.1 %) in He on the $Pt/Ce_{0.6}Zr_{0.2}Ca_{0.2}O_{1.8}F_x$ sample at 500°C . The sample weight is 0.516 g, feed rate is 40 cm^3/min. The figure legend: Sel. – selectivity of methane conversion into CO or CO_2; Red. CO, Red. CO_2 and Sum. Red. – degree of the sample reduction (in monolayers) corresponding to the surface oxygen consumption for methane oxidation into CO + H_2 or CO_2 + H_2O and sum of products, respectively; Conv. – degree of the reagents conversion

Sample reoxidation by water yielding more hydrogen proceeds rapidly and practically restores the reactive lattice oxygen capacity (Fig. 2). The same is true with respect to another mild oxidant like carbon dioxide (CO is generated in this case), and no specificity of the reduction curves is observed for the samples reoxidized by any of those reagents (Fig. 3). Note also that the reoxidation of the samples restores their reactivity. In the temperature and reagent concentration ranges studied, no deterioration of the samples in those reversible redox cycles (up to 5 cycles at 500°C) was detected.

Acknowledgments. This work was supported in part by RFBR-INTAS grant No. IR-97-402.

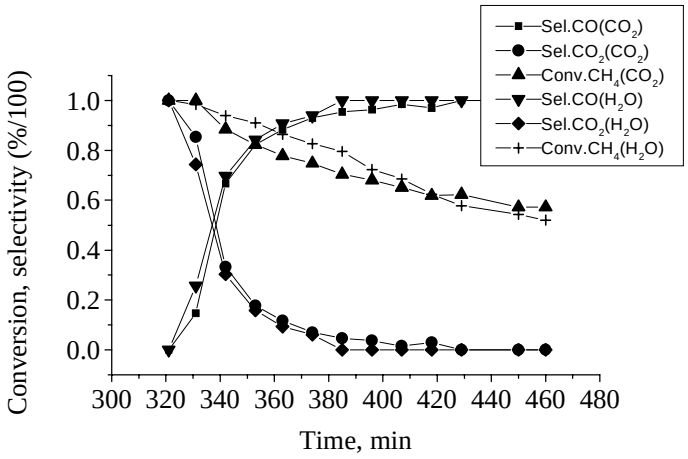

Fig. 3. Reduction of the $Pt/Ce_{0.6}Zr_{0.2}Ca_{0.2}O_{1.8}F_x$ sample at 500°C by 0.1 % CH_4 in He after the sample reoxidation by CO_2- and H_2O-containing mixtures. The figure legend: abbreviations are the same as in Fig. 2, the nature of mild oxidant is indicated in parentheses

REFERENCES

1. K. Otsuka, E. Sunada, T. Ushiyama, I. Yamanaka: *Stud. Surf. Sci. Catal.*, **107,** 531 (1997).
2. M. Fathi, F. Monnet, Y. Schuurman, A. Holmen, C. Mirodatos: *J. Catal.*, **190,** 439 (2000).
3. J. Kaspar, P. Fornasiero, M. Graziani: *Catal. Today*, **50**, 285 (1999).
4. M.P. Pechini: *U.S. Patent* 3,330,697.
5. M.G. Francesconi, P.R. Slater, J.P. Hodges, C. Greaves, P.P. Edwards, M. Al-Mamouri, M. Slaski: *J. Solid State Chem.*, **135,** 17 (1998).
6. S.N. Pavlova, V.A. Sadykov, V.A. Razdobarov, E.A. Paukshtis: *J. Catal.*, **161**, 507 (1996).
7. Ñ.E. Hori, H. Permana, K.Y.S. Ng, A. Brenner, K. More, K.M. Rahmoeller, D. Belton: *Appl. Catal. B: Envir.*, **16,** 105 (1998).
8. G. Vlaic, R. Di Monte, S. Geremia, J. Kaspar, M. Graziani: *J. Catal.*, **168,** 386 (1997).
9. L.L. Murrell, S.J. Tauster, D.R. Anderson, in *Proc. 10th Intern. Congr. Catal.*, Budapest, 19-24 July, 1992, L. Guczi, F. Solymosi, P. Tétényi eds., p. 681, Akadémiai Kiadó, Budapest, Hungary, 1993.
10. V.A. Drozdov, P.G. Tsyrulnikov, A.N. Pestryakov, A.A. Davydov: *Kinet. Katal.*, **29**, 484 (1988).
11. A.Ya. Rozovskii: *Catalyst and Reaction Media*, Nauka, Moscow, 1988.
12. Y. Madier, C. Descorme, A.M. Le Govic, D. Duprez: *J. Phys. Chem. B.*, **103**, 10999 (1999).
13. G. Balducci, J. Kaspar, P. Fornaiero, M. Graziani: *J. Phys. Chem. B.*, **101,** 1750 (1997).